Botanical Studies (2012) 53: 9-17.

Lemon ascorbate peroxidase: cDNA cloning and biochemical characterization

Ya-Han DAI[1,3,4], Chich-Yu HUANG[1,4], Lisa WEN[2,4], Dey-Chyi SHEU[3], and Chi-Tsai LIN[1,*]

[1]*Institute of Bioscience and Biotechnology and Center for Marine Bioenvironment and Biotechnology, National Taiwan Ocean University, Keelung 202, Taiwan*
[2]*Department of Chemistry, Western Illinois University, 1 University Circle, Macomb, IL 61455-1390, USA*
[3]*Department of Bioengineering, Tatung University, Taipei 104, Taiwan*

(Received October 27, 2010; Accepted June 24, 2011)

ABSTRACT. Ascorbate peroxidase (Apx) plays important roles both as a reductant and as a H_2O_2 scavenger via ascorbate (AsA). In this paper, we discuss how a ClApx cDNA (1,068 bp, GQ465430) encoding a putative Apx was cloned from lemon (*Citrus limon*). The deduced amino acid sequence is similar to the Apxes from other plant species. A 3-D structural model of ClApx was constructed based on the crystal structure of *Pisum sativum* Apx (PDB code 1APX). To characterize the ClApx protein, the coding region was subcloned into an expression vector pYEX-S1 and transformed into *Saccharomyces cerevisiae*. The recombinant His6-tagged ClApx was overexpressed and purified by Ni^{2+}-nitrilotriacetic acid Sepharose. The purified enzyme showed two prominent bands on 15% sodium dodecyl sulfate-polyacrylamide gel electrophoresis. The Michaelis constant (K_M) values of the recombinant enzyme for AsA and H_2O_2 were 0.40 and 0.11 mM, respectively. The enzyme was active from pH range 6 to 8. The thermal inactivation of the enzyme showed a half-life of 6.5 min at 45°C, and its inactivation rate constant K_i was 1.1×10^{-1} min^{-1}. The enzyme retained 35% activity after chymotrypsin digestion at pH 8 and 37°C for 40 min.

Keywords: Ascorbate peroxidase; *Citrus limon*; *Saccharomyces cerevisiae*; Three-dimension structural model.

Abbreviations: AsA, ascorbate; **Apx,** ascorbate peroxidase; **IPTG,** isopropyl β-D-thiogalactopyranoside; **SDS-PAGE,** sodium dodecyl sulfate-polyacrylamide gel electrophoresis; **MDHA,** monodehydroascorbate; **PBS,** phosphate buffer saline.

INTRODUCTION

The antioxidant properties of ascorbate (AsA) are a major focus in both plant and animal metabolism research. AsA can protect plants and mammals against oxidative stress. In most cases, monodehydroascorbate (MDHA) is the primary oxidation product of AsA. In plants, the reaction catalyzed by AsA peroxidase (Apx) is a major source of MDHA, which scavenges hydrogen peroxide (H_2O_2) (Hossain et al., 1984; Barrows and Poulos, 2005; Lu et al., 2009), and thus aids catalase (Ken et al., 2008) and peroxiredoxin (Wen et al., 2007; Liau et al., 2010) in modulating hydrogen peroxide levels. Some people use lemons to eliminate excess melanin in their skin. The cosmetic effect may be attributed to AsA and superoxide dismutase (SOD), among others found in lemon.

H_2O_2 has been recognized as a cytotoxic agent and a crucial component of receptor signaling that serves as an intracellular messenger (Rhee, 1999; Thannickal and Fanburg, 2000; Wahid et al., 2007; Chen et al., 2009). Receptor-mediated production of H_2O_2 has been studied mostly in phagocytic leukocytes (Babior, 1999). In these cells, one electron reduction of O_2 by a multicomponent NADPH oxidase generates superoxides that are then enzymatically converted to H_2O_2. Recently, the intracellular generation of superoxides and H_2O_2 has also been detected in various nonphagocytic cells (Lambeth, 2004). Timely elimination of messengers after completion of their functions has been shown to be critical for cellular signaling (Rhee et al., 2005). H_2O_2 may be eliminated by catalase, glutathione peroxidase, and peroxiredoxin. The Apxes can scavenge H_2O_2 by oxidizing the abundant AsA in plant cells (Nakano and Asada, 1981). Crystal structures of two known Apxes, PsApx (*Pisum sativum,* PDB code 1APX; Patterson and Poulos, 1995) and GmApx (*Glycine max*, PDB code 1OAG; Sharp et al., 2003) have been determined. Thus, Apxes play important roles in eliminating/detoxifying peroxides. Our aim is to study various lemon enzymes involved in modulating H_2O_2. Here, we report the cloning of an Apx (designated as ClApx) from lemon. The

[4]Footnote: The first and the second authors contributed equally to this paper.

*Corresponding author: E-mail: B0220@mail.ntou.edu.tw; Phone: 886-2-24622192 ext. 5513; Fax: 886-2-24622320.

coding region of the ClApx cDNA was introduced into a yeast expression system and the active enzyme was purified and characterized.

MATERIALS AND METHODS

Total RNA preparation from lemon and cDNA synthesis

A fresh unpeeled lemon (2.3 g) was obtained from a local market, frozen in liquid nitrogen, and ground to powder in a ceramic mortar. PolyA mRNA (30 μg) was prepared using Straight A's mRNA Isolation System (Novagen, USA). Four μg of the mRNA were used in the 5′-RACE-Ready cDNA and 3′-RACE-Ready cDNA syntheses with Clontech's SMART RACE cDNA Amplification Kit.

Apx cDNA isolation

A 0.65 kb fragment was amplified by PCR using the lemon 3′-RACE-Ready cDNA as a template and a UPM (universal primer A mix, purchased from BD Biosciences) primer & degenerate primer (5′ GAR GGY CGT CTT CCT GAT GC 3′), The degenerate primer was designed based on the conserved Apx sequences from CpApx (*Carica papaya*, EF512304), ZmApx (*Zea mays*, FJ890983), PpApx (*Pinus pinaster,* AY485994), AtApx (*Arabidopsis thaliana*, D14442), OsApx (*Oryza sativa*, D45423), CaApx (*Capsicum annuum*, AF442387), and AmApx (*Avicennia marina*, EU025130). The 0.65 kb fragment was subcloned and sequenced. Based on this DNA sequence, we synthesized an Apx-3R primer (5′ CCA TCC TTC TCA CCA GTC 3′). The primer allowed sequence extension from the 5′ end of the 0.65 kb fragment. A PCR was carried out using 0.2 μg of the 5′-RACE-Ready cDNA as a template. The primer pairs were UPM and Apx-3R primer. A 0.7 kb fragment (5′-RACE; 5′-DNA end) was amplified. The 0.7 kb DNA fragment was subcloned into pCR4 vector and transformed into *Escherichia coli* TOPO10. The nucleotide sequence of this insert was determined in both strands. Sequence analysis revealed that the combined sequences covered an open reading frame of a putative ClApx cDNA (1068 bp, GQ465430).

ClApx sequence bioinformatics analysis

The identity of the ClApx cDNA clone was verified by comparing the DNA sequence and the inferred amino acid sequence with various data banks using the basic local alignment search tool (BLAST). Multiple alignments were constructed using the ClustalW2 program. Protein secondary structure was predicted by the SWISS-MODEL program and represented as α helices and β strands. A 3-D structural model of ClApx was constructed by SWISS-MODEL (Arnold et al., 2006) (http://swissmodel.expasy.org/ SWISS-MODEL.html) based on the known crystal structure of PsApx (*Pisum sativum,* PDB ID: 1APX). The model was then superimposed onto GmApx (*Glycine max*, PDB ID: 1OAG) via the SPDBV_4 program. To study the ClApx evolutionary relationships among plant Apx sequences, a phylogenetic analysis was performed using Phylip-3.69 program (http://evolution.genetics.washington.edu/ phylip.html) via the Maximum Likelihood (ML) phylogenetic tree.

ClApx cDNA subcloning into an expression vector

The coding region of the ClApx cDNA was amplified using gene specific flanking primers. The 5′ upstream primer contains the *Eco*RI recognition site (5′ GAA TTC GAT GAC GAA GAA TTA CCC CAC 3′) and the 3′ downstream primer contains the *Xho*I recognition site (5′ CTCGAG GGC TTC AGC AAA TCC TAG CT 3′). Using 0.2 μg of 5′-RACE-ready cDNA as a template, and 10 pmole of each 5′ upstream and 3′ downstream primers, a 0.75 kb fragment was amplified by PCR. The fragment was ligated into pCR4 and transformed into *E. coli*. The recombinant plasmid was isolated and digested with *Eco*RI and *Xho*I after which the digestion products were separated on a 1% agarose gel. The 0.75 kb insert DNA was gel purified and subcloned into the *Eco*RI and *Xho*I sites of pET-20b(+) expression vector (Novagen). The recombinant DNA (pET-20b(+)-ClApx) was then transformed into *E. coli* C41(DE3). The recombinant protein was not overexpressed in the *E. coli* expression system. We decided to subclone the gene into a yeast expression system. The coding region of the ClApx cDNA was re-amplified by using two gene-specific primers: the 5′ upstream primer was the same whereas the 3′ downstream primer contained a His6-tag and *Eco*RI recognition site (5′ CGT CTC GAA TTC TCA GTG GTG GTG GTG GTG GTG 3′). Using the 0.1 μg recombinant DNA of pET-20b(+)-ClApx as a template, and 10 pmole of each 5′ upstream and 3′ downstream primers, a 0.75 kb fragment was amplified by PCR. The fragment was ligated into pCR4 and transformed into *E. coli*. The recombinant plasmid was isolated and digested with *Eco*RI and the digestion products were separated on an 0.8% agarose gel. The 0.75 kb insert DNA was gel purified and subcloned into the *Eco*RI site of the pYEX-S1 expression vector (Clontech) and introduced into *Saccharomyces cerevisiae* (trp^- ura^-). The transformed yeast cells were selected by YNBDT (0.17% yeast nitrogen base, 0.5% ammonium sulfate, and 2% glucose) agar plates containing 20 μg Trp/mL. The presence of ClApx cDNA in the selected transformants was verified by PCR using gene-specific flanking primers. The recombinant ClApx protein was expressed in yeast in YPD medium (1% yeast extract, 2% peptone, 2% glucose). Active recombinant ClApx production was shown using an enzyme assay.

Recombinant ClApx expression and purification

The transformed yeast containing the ClApx was grown at 30°C in 250 mL of YPD medium for 5 days. The cells were harvested and soluble proteins extracted in PBS with glass beads as previously described (Huang et al., 2010a, b). The recombinant ClApx was purified by Ni-NTA affinity chromatography (elution buffer: 30% PBS

containing 100 mM imidazole) according to the manufacture's instruction (Qiagen). The purified protein was checked by 15% SDS-PAGE. Proteins on the gel were detected by Coomassie Brilliant Blue R-250 staining. Protein concentration was determined using a Bio-Rad Protein Assay Kit (Richmond, CA) using bovine serum albumin as a standard.

Electrospray ionization quadrupole-time-of-flight (ESI Q-TOF) molecular mass analysis

The purified recombinant ClApx (0.1 mg/mL) was dissolved in 3% PBS containing 0.05 mM imidazole and 0.5% glycerol. The sample (5 µL) was used for molecular mass determination using an ESI Q-TOF mass spectrometer (Micromass, Manchester, England).

Apx activity assay and kinetic studies

Apx activity was determined by measuring AsA oxidation (Nakano and Asada, 1981). The reaction mixture (100 µL) contained 20 mM potassium phosphate (pH 7.4), 1 mM H_2O_2, 1 mM AsA and 0.2 µg ClApx. The reaction started upon the addition of ClApx. The reaction was followed by a decrease in A_{290} due to AsA oxidation.

ClApx (0.2 µg) kinetic properties were determined by varying the concentrations of AsA (0.06 to 1.0 mM) with the fixed amount of 1 mM H_2O_2 or varying concentrations of H_2O_2 (0.06 to 1.0 mM) with the fixed amount of 1 mM AsA. The change in absorbance at 290 nm was recorded between 10 sec and 20 sec. The molar absorption coefficient of AsA at 290 nm was 2.8 mM^{-1} cm^{-1}. The K_M, V_{max} and k_{cat} were calculated from Lineweaver-Burk plots.

Biochemical characterization

The stability of ClApx under various conditions was studied by assaying its peroxidase activity. Aliquots of the ClApx sample were tested for: (1) *Thermal effect*. Enzyme sample (0.2 µg/2 µL enzyme in 3% PBS containing 5% glycerol per reaction) was heated to 45°C for 2, 4, 8 or 16 min. (2) *pH effect*. Enzyme sample (0.2 µg/2 µL enzyme in 3% PBS containing 5% glycerol per reaction) was adjusted to the desired pH by adding a volume of buffer with different pHs: 0.2 M citrate buffer (pH 2.5, 4.0), 0.2 M potassium phosphate buffer (pH 6.0, 7.0 or 8.0) or 0.2 M CAPS buffer (pH 10.4, or 11.0). Each sample was incubated at 37°C for 1 h. (3) *Imidazole effect*. During protein purification, the ClApx enzyme was eluted with imidazole and its effect on activity was examined. Imidazole was added to the enzyme sample (0.2 µg/2 µL enzyme in 3% PBS containing 5% glycerol per reaction) to the final levels (each final volume is 20 µL) of 0.2, 0.4, or 0.8 M and incubated at 37°C for 1 h. (4) *Proteolytic susceptibility.* The enzyme (1.0 µg/10 µL in 1.5 % PBS containing 2.5% glycerol, additional 10 mM $CaCl_2$ for chymotrypsin) was incubated with one-tenth of trypsin or chymotrypsin (w/w) at pH 8.0, 37°C for a period of 5, 10, 20 or 40 min. Aliquots (0.2 µg/2 µL) were removed at various time intervals for analysis. After each treatment, the residue Apx activity was tested as described above.

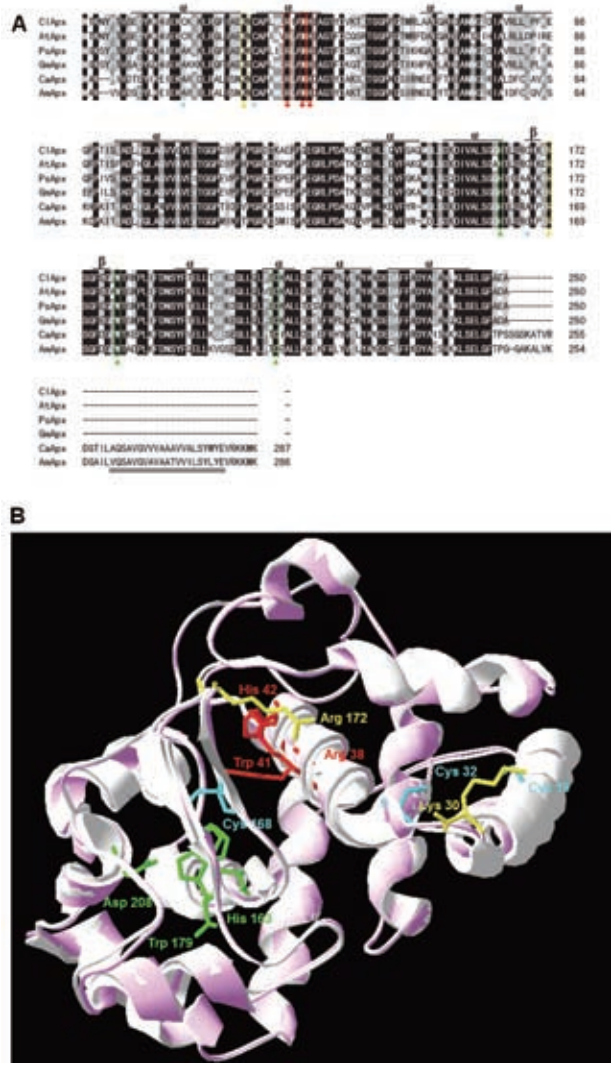

Figure 1. Alignment of the ClApx amino acid sequences with other organism's Apxes and 3-D structural model. (A) Sequence alignment: ClApx (this study), AtApx (*Arabidopsis thaliana*), PsApx (*Pisum sativum*), GmApx (*Glycine max*), CaApx (*Capsicum annuum*) and AmApx (*Avicennia marina*). Conservative replacements are shaded gray. Protein secondary structure was predicted by the SWISS-MODEL program and predicted α helices and β strands are indicated; (B) A 3-D structural model of ClApx was modeled based on the known X-ray structure of PsApx (*Pisum sativum*) via the SWISS-MODEL program and was superimposed to obtain a better structure via the SPDBV_4 program. Superimposition of ClApx (pink) and GmApx (*Glycine max*) (white) was shown using protein solid ribbons. Blue stars denote the 3 Cys residues in the ClApx protein. The yellow triangles indicate the putative AsA binding sites. The red triangles indicate the putative active sites. The green triangles denote the conserved residues of the putative proximal hydrogen bonded triad. Double underline denote the C-terminal membrane-spanning segment belonging to **cm**1 type.

RESULTS

Cloning and characterization of a cDNA encoding ClApx

A putative ClApx cDNA clone was identified based on its sequence homology to the published Apxes in the NCBI data bank. The coding region of ClApx cDNA was 750 bp that encodes a protein of 250 amino acid residues with calculated molecular mass of 29 kDa (EMBL accession no. GQ465430). Theoretical pI/Mw was 5.6/27570. Figure 1 shows the optimal alignment of the ClApx amino acid sequences with five related Apx sequences from other sources. ClApx is most similar (80%) to AtApx (*Arabidopsis thaliana*, BAA03334), PsApx (*Pisum sativum,* P48534) and GmApx (*Glycine max*, Q43758), and 60% similar to CaApx (*Capsicum annuum*, AF442387) and AmApx (*Avi-*

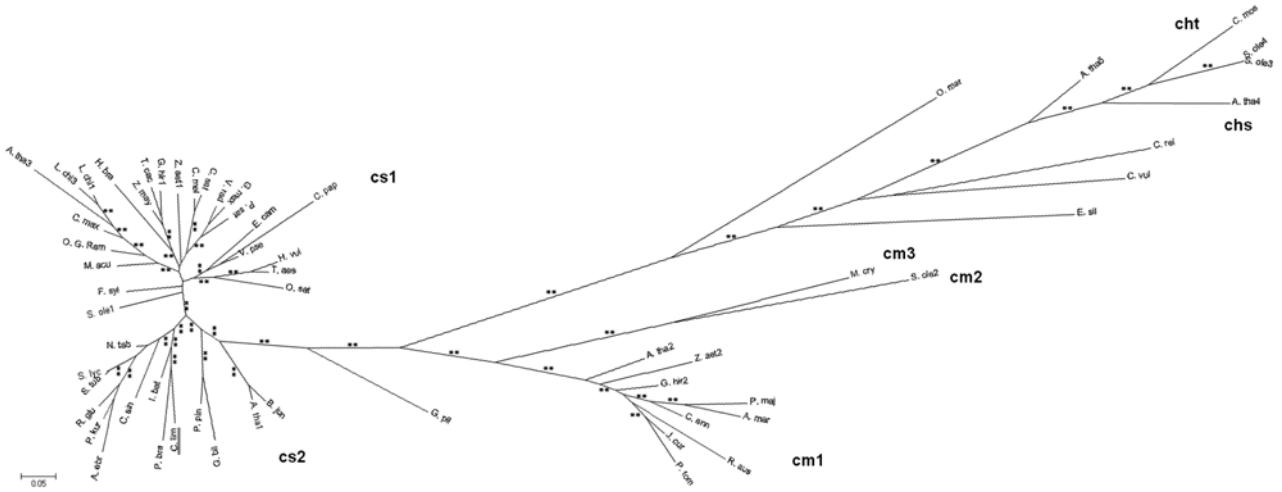

Figure 2. Phylogenetic tree showing the relationships among plant Apxes. The sources of the ascorbate peroxidase sequences including species, abbreviations, accession numbers, enzyme types, and number of amino acids are shown in Table 1. The tree was made using the Phylip-3.69 program (http://evolution.genetics.washington.edu/phylip.html) via Maximum Likelihood (ML) phylogenetic tree. The ML method is a statistical method and a p value is provided for each branch. The right branches of the tree, **cht** (thylakoid-bound), chs (stroma-bound), **cm** (cytosol membrane-bound)**1**, **cm2**, and **cm3** ascorbate peroxidases, represent the evolution of these 14 plant species. The upper left branch of the tree, the cytosol-souble (**cs1**) ascorbate peroxidases, represents the evolution of these 24 plant species. The lower left branch of the tree, the cytosol-souble (**cs2**) ascorbate peroxidases, represents the evolution of these 14 plant species including this study, *Citrus limon* (double underlines). ** denotes significantly different, $P < 0.01$.

Table 1. Sources of the ascorbate peroxidase sequences.

Species	Accession no.	Type	Numer of a. a.
Arabidopsis thaliana (A. tha3)	CAA56340	cs1	251
Carica papaya (C. pap)	ABS01350		250
Citrus maxima (C. max)	ABS42984		250
Cucumis melo (C. mel)	ABS42984		249
Cucumis sativus (C. sat)	ADT80721		249
Eucalyptus camaldulensis (E. cam)	ABH10015		227
Fagus sylvatica (F. syl)	CBY92008		192
Glycine max (G. max)	AAA61779		250
Gossypium hirsutum (G. hir1)	ACJ11731		250
Hevea brasiliensis (H. bra)	AAO14118		250
Hordeum vulgare (H. vul)	AAL08496		256
Litchi chinensis (L. chi3)	ABP57220		214
Litchi chinensis (L. chi1)	ABZ79406		250
Musa acuminata (M. acu)	ADK25940		203
Oncidium Gower Ramsey (O. G. Ram)	ACJ38537		249
Oryza sativa (O. sat)	BAA08264		250
Pisum sativum (P. sat)	AAA33645		250
Spinacia oleracea (S. ole1)	AAA99518		250
Theobroma cacao (T. cac)	ABR68691		250
Triticum aestivum (T. aes)	ACO90196		243
Vigna radiata (V. rad)	ACD44387		209
Vitis pseudoreticulata (V. pse)	AAZ79357		250
Zantedeschia aethiopica (Z. aet1)	AAK57005		250
Zea mays (Z. may)	ACO90192		250
Arabidopsis thaliana (A. tha4)	X98926	cht	425
Spinacia oleracea (S. ole3)	D77997		415
Cucurbita moschata (C. mos)	D83656		421
Arabidopsis thaliana (A. tha5)	X98925	chs	372
Spinacia oleracea (S. ole4)	D83669		365

Species	Accession no.	Type	Numer of a. a.
Acanthus ebracteatus (A. ebr)	ABK32072	cs2	250
Arabidopsis thaliana (A. tha1)	BAA03334		250
Brassica juncea (B. jun)	AAN60795		250
Camellia sinensis (C. sin)	ACB45429		250
Citrus limon (C. lim, this work)	GQ465430		250
Ginkgo biloba (G. bil)	ACL81497		251
Ipomoea batatas (I. bat)	AAP42501		250
Nicotiana tabacum (N. tab)	AAA86689		250
Picrorhiza kurrooa (P. kur)	ACF93235		250
Pimpinella brachycarpa (P. bra)	AAF22246		250
Pinus pinaster (P. pin)	AAR32786		249
Rehmannia glutinosa (R.. glu)	AAS19934		250
Solanum lycopersicum (S. lyc)	AAX84654		250
Solanum tuberosum (S. tub)	BAC22953		250
Arabidopsis thaliana (A. tha2)	CAA66640	cm1	287
Avicennia marina (A. mar)	ABS82577		286
Capsicum annuum (C. ann)	AAL35365		287
Gossypium hirsutum (G. hir2)	AAB52954		288
Jatropha curca (J. cur)	ACT87980		288
Plantago major (P. maj)	CAH59427		289
Populus tomentosa (P. tom)	AAV58827		286
Rheum australe (R. aus)	AAY90125		285
Zantedeschia aethiopica (Z. aet2)	AAD43334		288
Spinacia oleracea (S. ole2)	BAA08535	cm2	309
Mesembryanthemum crystallinum (M. cry)	AAA86262	cm3	260
Chlamydomonas reinhardtii (C. rei)	CAA11265	unknown	327
Chlorella vulgaris (C. vul)	AAY51484		264
Ectocarpus siliculosus (E. sil)	CBJ27103		257
Grimmia pilifera (G. pil)	ADF56044		256
Oxyrrhis marina (O. mar)	ACE81819		311

cennia marina, EU025130). Like all other Apx sequences, the ClApx sequence contained no signal peptides and appeared to be cytosolic. We predicted the secondary structure (Figure 1A, represented as α helices and β strands) and a 3-D structural model (Figure 1B, represented as solid ribbon) using SWISS-MODEL program. The 3-D structural model was constructed based on the known crystal structure of PsApx (*Pisum sativum*). The model (pink) was superimposed onto GmApx (*Glycine max*) (white) via the SPDBV_4 program. Figure 1A and B show several color coded conserved residues presumably involved in various important functions. Blue stars denote the 3 Cys residues ($Cys^{19, 32, 168}$) in the ClApx protein. The Cys^{32} is totally conserved and is located near the AsA binding site based on the 3-D structural model (Figure 1B). The yellow triangles denote the putative AsA binding sites (Lys^{30}, Arg^{172}) (Macdonald et al., 2006). The red triangles denote the putative active sites (Arg^{38}, Trp^{41}, His^{42}) (Efimov et al., 2007). The green triangles denote the conserved residues of the putative proximal hydrogen bonded triad (His^{163}, Asp^{208}, Trp^{179}) (Barrows and Poulos, 2005), and the ClApx belongs to heme peroxidase. Its Trp^{179} in the proximal heme pocket may form the more traditional porphyrin *ð*-cation radical (Barrows and Poulos, 2005). The heme propionates play a role in stabilization of porphyrin *ð*-cation radicals. Using density functional theory, Guallar et al. (2003) reported that protecting the propionate groups by forming hydrogen bonds with the nearby residues is responsible for stabilization of a porphyrin *ð*-cation radical.

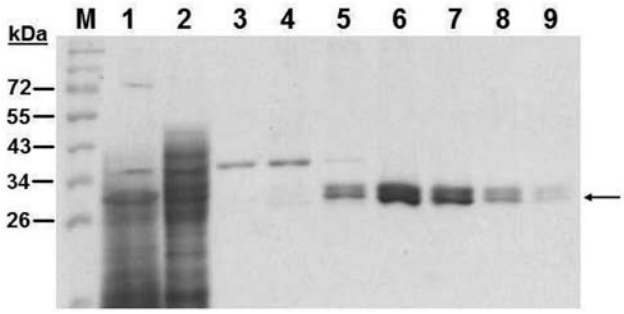

Figure 3. Expression and purification of recombinant ClApx in yeast. Fifteen μL (loading buffer without β-mercaptoethanol and without boiling) of each fraction was loaded into each lane of the 15% SDS-PAGE. Lane 1, crude extract from yeast expressing ClApx; 2, flow-through proteins from the Ni-NTA column (2 mL); 3-4, washed from Ni-NTA column; 5-9, ClApx (each fraction was 1.5 mL) eluted from Ni-NTA column. Molecular masses (in kDa) of standards are shown at left. Arrow indicated the target protein.

Through sequence analysis, Jespersen et al. (1997) classified plant Apxes (sequences from 20 species) into seven types based on differences in their cellular locations and their structural characteristics: **cs1** (cytosol soluble 1), **cs2, cm1 (**cytosol membrane-bound 1), **cm2, cm3, chs** (chloroplast stroma), and **cht (**chloroplast thylakoid-bound). The analysis was expanded in this study to include all new plant Apx sequences published from 1997 to the present, including the ClApx (Table 1). A phylogenetic tree was generated (Figure 2) using the same classification and the ML phylogenetic analysis of the 59 plant species of the Apx sequences. The p values at each branch donated by ** were less than 0.01, and were thus *significantly* different. This ClApx appeared to belong to the **cs2** type.

Recombinant ClApx expression and purification

The ClApx (0.75 kb) coding region was amplified by PCR and subcloned into a yeast expression vector, pYEX-S1, as described in the Materials and Methods section. Positive clones were verified by DNA sequence analysis. The recombinant ClApx was expressed, and the proteins were analyzed on a 15% SDS-PAGE in the absence a reducing agent without boiling (Figure 3). The recombinant ClApx was expressed as a His6-tagged fusion protein and was purified by affinity chromatography with nickel-chelating Sepharose. The purified ClApx protein appeared as double bands on SDS-PAGE and had a molecular mass of ~29 kDa (expected size of ClApx) (Figure 3, lanes 5-9). Analysis of the ClApx by ESI Q-TOF confirmed the pres-

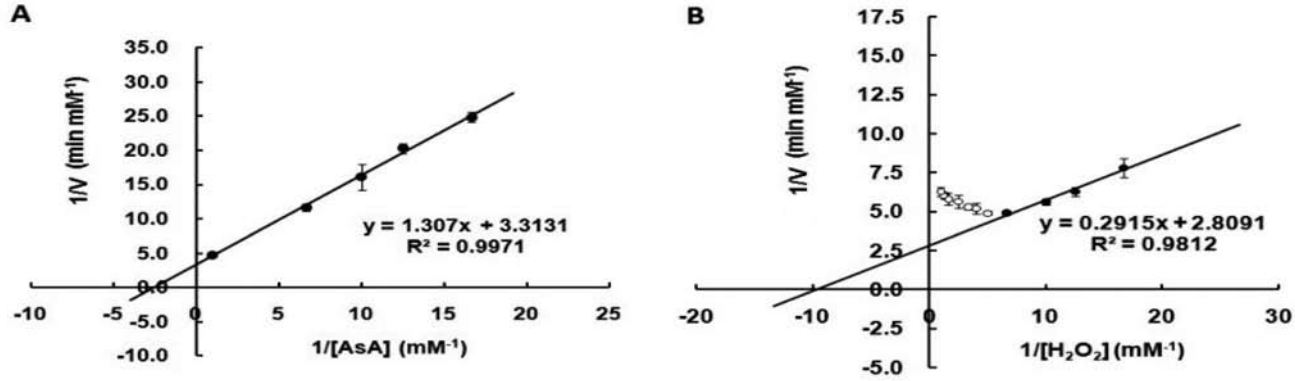

Figure 4. Double-reciprocal plots of varying AsA and H_2O_2 concentrations on ClApx activity. The initial rate of the enzymatic reaction was measured at 1 mM H_2O_2 with the AsA concentration varied from 0.06 to 1.0 mM (A). The activities were also measured at 1.0 mM AsA with the H_2O_2 concentration varied from 0.06 to 1.0 mM (B). The K_M, $V_{max,}$ and k_{cat} were calculated from the Lineweaver-Burk plots.

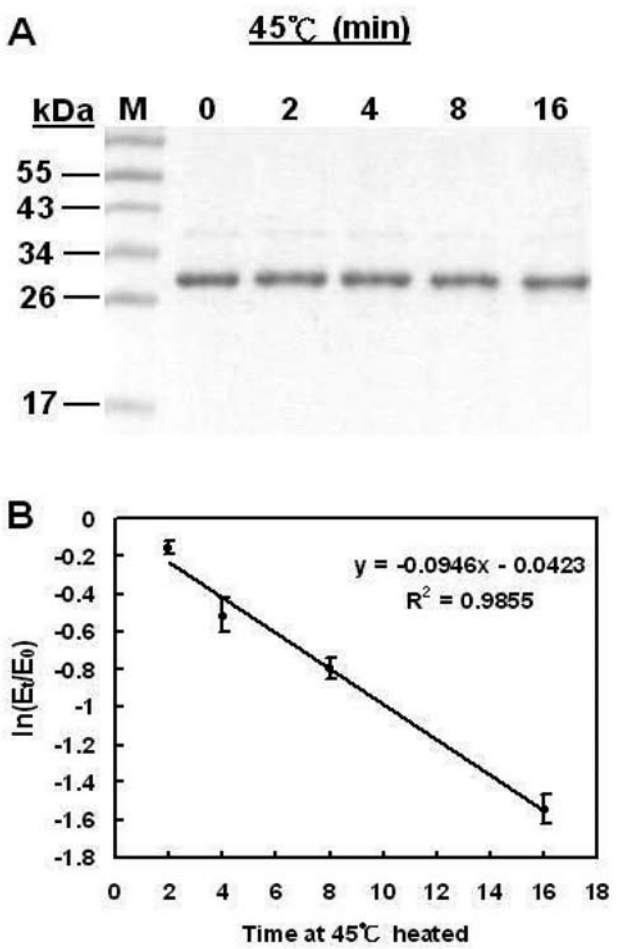

Figure 5. Effect of temperature on the purified ClApx. The enzyme sample was heated at 45°C for various time intervals. Aliquots of the sample were taken at 0, 2, 4, 8 or 16 min and analyzed by SDS-PAGE (A) and assayed for Apx activity. The thermal inactivation kinetics of ClApx activity was plotted (B). E_0 and E_t are original activity and residual activity after being heated for different time intervals. Data are means of three experiments.

ence of a major protein of 28.1 kDa. This indicated that the enzyme was predominantly monomeric in solution. The Ni-NTA-eluted fractions were pooled and characterized further. The yield of the purified His6-tagged ClApx was 930 μg from 150 mL of culture. Functional ClApx was detected by an activity assay as describe below.

Recombinant ClApx characterization and kinetic studies

The recombinant ClApx was used to catalyze the conversion of AsA to MDHA. Figure 4 shows the AsA consumption in the presence of H_2O_2 (1 mM) and purified ClApx (0.2 μg/0.1 mL). The electrons produced in the reaction were used to reduce H_2O_2 into H_2O. As shown in Figure 4A-B, the Lineweaver-Burk plot of the velocity (1/V) against 1/[AsA] gave the K_M = 0.40 mM, V_{max} = 0.29 mM/min, and k_{cat} = 4.2 × 10^3 min^{-1}. The plot of the velocity (1/V) against 1/ [H_2O_2] gave the K_M = 0.11 mM, V_{max} = 0.36 mM/min, and k_{cat} = 5.1 × 10^3 min^{-1} for the ClApx, respectively.

ClApx thermal stability and imidazole effects were tested because the information was considered useful for developing enzyme purification protocols. To examine the effect of high temperature on the ClApx activity, the enzyme was treated as described in the Materials and Methods section and then analyzed for Apx activity residue. The ClApx's half-life of inactivation at 45°C was 6.5 min, and its thermal inactivation rate constant K_i was 1.1 × 10^{-1} min^{-1} (Figure 5). The ClApx has an optimal Apx activity at pH 7.0, and the enzyme retained significant activity at pHs 6.0-8.0 (Figure 6A). The enzyme showed a decrease in its activity with increasing imidazole concentration from 0-0.8 M (Figure 6B). Approximately 50% activity was lost in the presence of 0.8 M imidazole. The enzyme lost 65% activity after 40 min of incubation at 37°C with one-tenth its weight of chymotrypsin (Figure 6C). However, the enzyme retained all the activity after 40 min of incubation at 37°C with one-tenth its weight of trypsin (Figure 6C).

Table 2. Kinetic analyses of ClApx and the other two Apxes (from *P. tomentosa* and *C. pea*). The kinetic parameters were determined as described in the Materials and Methods. The K_M value for ascorbate (AsA) was determined at 0.06-1.0 mM AsA and 1.0 mM H_2O_2. The K_M value for H_2O_2 was determined at 0.06-1.0 mM H_2O_2 and 1.0 mM AsA. Data represent the mean (±SE) of three separate experiments.

		C. limon	*P. tomentosa*	*C. pea*
AsA	K_M (mM)	0.40 ± 0.03	0.53 ± 0.04	0.30 ± 0.03
	k_{cat} (min^{-1})	4.29 × 10^3	1.04 × 10^2	4.80 × 10^3
	k_{cat}/ K_M (min^{-1} mM^{-1})	1.07 × 10^4	1.97 × 10^2	1.60 × 10^4
H_2O_2	K_M (mM)	0.11 ± 0.03	0.12 ± 0.01	
	k_{cat} (min^{-1})	5.07 × 10^3	1.22 × 10^2	
	k_{cat}/ K_M (min^{-1} mM^{-1})	4.61 × 10^4	1.02 × 10^3	

Values are from this work [*C. limon* (ClApx)] or from the literature: *P. tomentosa* Apx (Lu et al., 2009) and *C. pea* Apx (Macdonald et al., 2006).

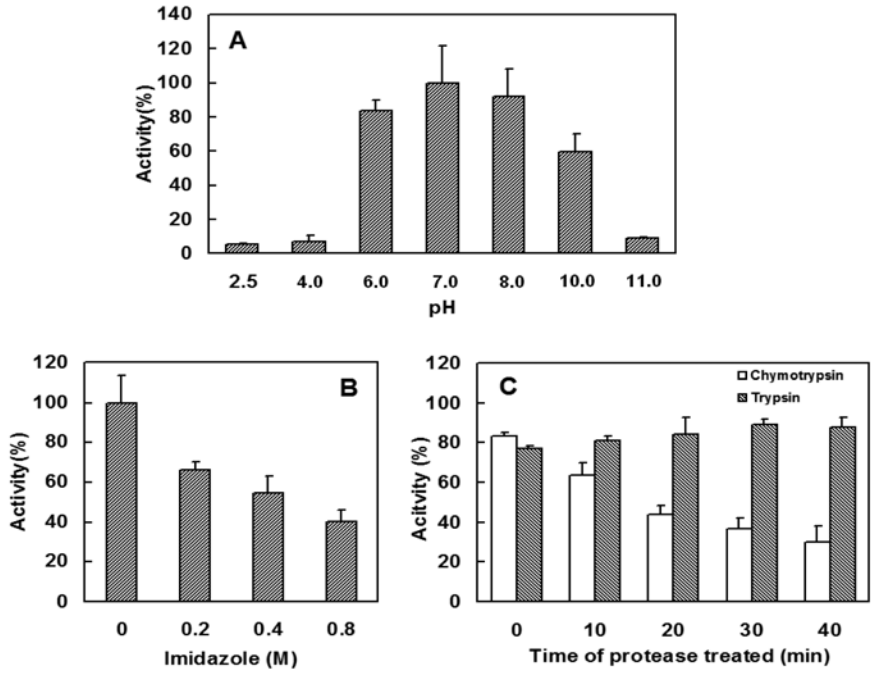

Figure 6. Effect of pH, imidazole, and chymotrypsin or trypsin on the purified ClApx. A, The enzyme samples were incubated with different pH buffer at 37°C for 1 h and then assayed for Apx activity; B, The enzyme samples were incubated with various concentration of imidazole at 37°C for 1 h and then checked for Apx activity; C, The enzyme samples were incubated with chymotrypsin or trypsin at 37°C for various time and then checked for Apx activity. Data are means of three experiments.

The protease test results will help us understand the effect of digestive enzymes on the ClApx and its suitability as a health food.

DISCUSSION

In the present study, we cloned, expressed, purified, and characterized a lemon Apx that plays important roles in scavenging H_2O_2. Based on the classification of plant Apxes (Jespersen et al., 1997) and the phylogenetic tree (Figure 2), the ClApx belongs to the **cs**2 type. Many oxidoreductase enzymes such as monodehydroascorbate reductase (Huang et al., 2010a, b), dithiol glutaredoxin (Ken et al., 2009), dehydroascorbate reductase (Jiang et al., 2008), and peroxiredoxins (Wen et al., 2007; Liau et al., 2010) possess Cys residues to catalyze its redox reaction. The ClApx enzyme (Figure 1) contains three Cys residues at the positions 19, 32 and 168. Cys^{32} is totally conserved in all six Apx enzymes as shown in Figure 1. It is possible that the Cys^{32} residue (near Lys^{30} which presumably binds AsA) participates in the transfer of electrons from AsA to catalyze the conversion of AsA to one electron oxidized form of the substrate (MDHA) and H_2O_2 to H_2O. Based on the structural model shown in Figure 1B, Cys^{19}, Cys^{32} and Cys^{168} may form an intramolecular disulfide bond between any two of these Cys residues due to their close proximity. It is possible that the lower band seen in the SDS-PAGE (Figure 3, lanes 5-9) represents the formation of a more compact ClApx with an intramolecular disulfide bond. Based on the PAGE analysis and the ESI Q-TOF data, the purified enzyme existed only in its monomeric form. This is similar to those of the stromal and thylakoid membrane-bound monomeric Apxs from most plants (Ishikawa et al., 1996), but different from the dimeric Apx from *Populus tomentosa* (Lu et al., 2009).

Furthermore, Macdonald et al. reported (2006) that the Apx catalytic mechanism involved formation of an oxidized Compound I intermediate that was subsequently reduced by the substrate (AsA) in two, successive single electron transfer steps [eqs 1-3, where HS (AsA) denotes substrate and $S^{\cdot}$ denotes one electron oxidized form of the substrate]

$$\text{Apx} + H_2O_2 \rightarrow \text{Compound I} + H_2O \quad (1)$$

$$\text{Compound I} + \text{HS} \rightarrow \text{Compound II} + S^{\cdot} \quad (2)$$

$$\text{Compound II} + \text{HS} \rightarrow \text{Apx} + S^{\cdot} + H_2O \quad (3)$$

Residues Lys^{30} and Arg^{172} of Apx enzymes are binding sites of the AsA. Apxes show high specificity for L-AsA but will also oxidize other nonphysiological substrates (Macdonald et al., 2006). ClApx also contains the same Lys^{30} and Arg^{172} residues and is expected to possess a similar mechanism of scavenging H_2O_2.

The ClApx appears to show substrate inhibition at high H_2O_2 concentration. As shown in Figure 4B, the Lineweaver-Burk plot showed the effects of substrate inhibition when the H_2O_2 concentration was over 0.2 mM. Further investigation is necessary to confirm whether H_2O_2 really can inhibit its own conversion to product at very high concentrations.

We compared the K_M and k_{cat} values of the ClApx for AsA with those of *P. tomentosa* Apx. As shown in Table 2, Lu et al. (2009) reported that *P. tomentosa* Apx had K_M and k_{cat} values of 0.53 mM and 1.22×10^2 min^{-1} for AsA. The lemon Apx has lower K_M (0.40 mM) and higher k_{cat} (4.2×10^3 min^{-1}) for AsA. Therefore, our results suggest that ClApx can scavenge H_2O_2 efficiently at a lower AsA concentration.

Acknowledgement. This work was supported by the National Science Council of the Republic of China, Taiwan under grant NSC 97-2313-B-019-001-MY3 to C-T. L.

LITERATURE CITED

Arnold, K., L. Bordoli, J. Kopp, and T. Schwede. 2006. The SWISS-MODEL workspace: a web-based environment for protein structure homology modeling. Bioinformatics **22:** 195-201.

Babior, B.M. 1999. NADPH oxidase: an update. Blood **93:** 1464-1476.

Barrows, T.P. and T.L. Poulos. 2005. Role of electrostatics and salt bridges in stabilizing the compound I radical in ascorbate peroxidase. Biochemistry **44:** 14062-14068.

Chen, X.Y., X. Ding, S. Xu, R. Wang, W. Xuan, Z.Y. Cao, J. Chen, H.H. Wu, M.B. Ye, and W.B. Shen. 2009. Endogenous hydrogen peroxide plays a positive role in the up-regulation of heme oxygenase and acclimation to oxidative stress in wheat seedling leaves. J. Integrat. Plant Biol. **51:** 951-960.

Efimov, I., N.D. Papadopoulou, K.J. McLean, S.K. Badyal, I.K. Macdonald, A.W. Munro, P.C. E. Moody, and E.L. Raven. 2007. The redox properties of ascorbate peroxidase. Biochemistry **46:** 8017-8023.

Guallar, V., M. H. Baik, S.J. Lippard, and R.A. Friesner. 2003. Peripheral heme substituents control the hydrogen-atom abstraction chemistry in cytochromes P450. Proc. Natl. Acad. Sci. USA **100:** 6998-7002.

Hossain, M.A., Y. Nakano, and K. Asada. 1984. Monodehydroascorbate reductase in spinach chloroplasts and its participation in regeneration of ascorbate for scavenging hydrogen peroxide. Plant Cell Physiol. **25:** 385-395.

Huang, C.Y., C.F. Ken, H.H. Chi, L. Wen, and C.T. Lin. 2010a. Cloning, expression and characterization of a thioredoxin reductase cDNA from *Taiwanofungus camphorate.* J. Agric. Food Chem. **58:** 4825-4830.

Huang, C.Y., L. Wen, R.H. Juang, D.C. Sheu, and C.T. Lin. 2010b. Monodehydroascorbate reductase cDNA from sweet potato: expression and kinetic studies. Bot. Stud. **51:** 37-44.

Ishikawa, T.S., K. Yoshimura, and K. Takeda. 1996. cDNAs encoding spinach stromal and thylakoid-bound ascorbate peroxidase, differing in the presence or absence of their 3′-coding regions. FEBS Lett. **384:** 289-293.

Jespersen, H.M., I.V.H. Kjaersgaird, L. Østergaard and K.G. Welinder. 1997. From sequence analysis of three novel ascorbate peroxidases from *Arabidopsis thaliana* to structure, function and evolution of seven types of ascorbate peroxidase. Biochem. J. **326:** 305-310.

Jiang, Y.C., C.Y. Huang, L. Wen, and C.T. Lin. 2008. Dehydroascorbate reductase cDNA from sweet potato (*Ipomoea batatas* [L.] Lam): expression, enzyme properties, and kinetic studies. J. Agric. Food Chem. **56:** 3623-3627.

Ken, C.F., H.T. Chen, R.C. Chang, and C.T. Lin. 2008. Biochemical characterization of a catalase from *Antrodia camphorata*: expression in *Escherichia coli* and enzyme properties. Bot. Stud. **49:** 119-125.

Ken, C.F., C.Y. Lin, Y.C. Jiang, L. Wen, and C.T. Lin. 2009. Cloning, expression and characterization of an enzyme possesses both glutaredoxin and dehydroascorbate reductase activity from *Taiwanofungus camphorata*. J. Agric. Food Chem. **57:** 10357-10362**.**

Lambeth, J.D. 2004. NOX enzymes and the biology of reactive oxygen. Nat. Rev. Immunol. **4:** 181-189.

Liau, Y.J., Y.T. Chen, C.Y. Lin, J.K. Huang, and C.T. Lin. 2010. Characterization of 2-Cys peroxiredoxin isozyme (Prx1) from *Taiwanofungus camphorata* (Niu-chang-chih): expression and enzyme properties. Food. Chem. **119:** 154-160.

Lu, H.R., L. Han, and X.N. Jiang. 2009. Heterologous expression and characterization of a proximal ascorbate peroxidase from *Populus tomentosa.* Mol. Biol. Rep. **36:** 21-27.

Macdonald, I.K., S.K. Badyal, L. Ghamsari, P.C.E. Moody, and E.L. Raven. 2006. Interaction of ascorbate peroxidase with substrates: A mechanistic and structural analysis. Biochemistry **45:** 7808-7817.

Nakano, Y. and K. Asada. 1981. Hydrogen peroxide is scavenged by ascorbate-specific peroxidase in spinach chloroplasts. Plant Cell Physiol. **22:** 867-880.

Patterson, W.R. and T.L. Poulos. 1995. Crystal structure of recombinant pea cytosolic ascorbate peroxidase. Biochemistry **34:** 4331-4341.

Rhee, S.G. 1999. Redox signaling: Hydrogen peroxide as intracellular messenger. Exp. Mol. Med. **31:** 53-59.

Rhee, S.G., K.S. Yang, S.W. Kang, H.A. Woo, and T.S. Chang. 2005. Controlled elimination of intracellular H_2O_2: regulation of peroxiredoxin, catalase, and glutathione peroxidase via post-translational modification. Antioxid. & Redox Signaling. **7:** 619-626.

Sharp, K.H., M. Mewies, P.C. Moody, and E.L. Raven. 2003. Crystal structure of the ascorbate peroxidase-ascorbate complex. Nat. Struct. Biol. **10:** 303-307.

Thannickal, V.J. and B.L. Fanburg. 2000. Reactive oxygen species in cell signaling. Am. J. Physiol. Lung Cell Mol. Physiol. **279:** L1005-L1028.

Wahid, A., M. Perveen, S. Gelani, and S.M. Basra. 2007. Pretreatment of seed with H_2O_2 improves salt tolerance of wheat seedlings by alleviation of oxidative damage and expression of stress proteins. J. Plant Physiol. **164:** 283-294.

Wen, L., H.M. Huang, R.H. Juang, and C.T. Lin. 2007. Biochemical characterization of 1-Cys peroxiredoxin from *Antrodia camphorata*. Appl. Microbiol. Biotechnol. **73:** 1314-1322.

檸檬抗壞血酸過氧化酶選殖及生化特性研究

戴亞涵[1, 3] 黃智郁[1] 溫麗莎[2] 許垤基[3] 林棋財[1]

[1] 國立台灣海洋大學 生物科技研究所
[2] 美國 Western Illinois 大學 化學系
[3] 大同大學 生物工程學系

抗壞血酸過氧化酶 (Ascorbate peroxidase, Apx) 扮演氧化抗壞血酸 (AsA) 以清除過氧化氧 (H_2O_2)。從檸檬 (*Citrus limon*) cDNA 庫選殖出 Apx cDNA 序列 (1,068 bp, GQ465430)，全長共 1,068 個核苷酸，可轉譯出 250 個胺基酸。經序列比較 ClApx 與其他物種的序列有很高的相似性，依據已知結構，建立一模擬立體結構 (3-D structural model)。在演化樹上屬於 **cs2** (cytosol soluble)。進一步將其轉譯區選殖入表現載體 pYEX-S1，以酵母菌 *Saccharomyces cerevisiae* 作爲表現宿主，經親和性管柱純化可得到具有活性的 ClApx，對 AsA 和 H_2O_2 其 K_M 值分別爲 0.40 和 0.11 mM。其特性在 45°C 加熱活性降低一半的時間爲 6.5 分鐘，在 pH 6.0 ~ 8.0 仍然具有相當的活性。

關鍵詞：檸檬；抗壞血酸過氧化酶；模擬立體結構；酵母菌。